ChemComm

Accepted Manuscript

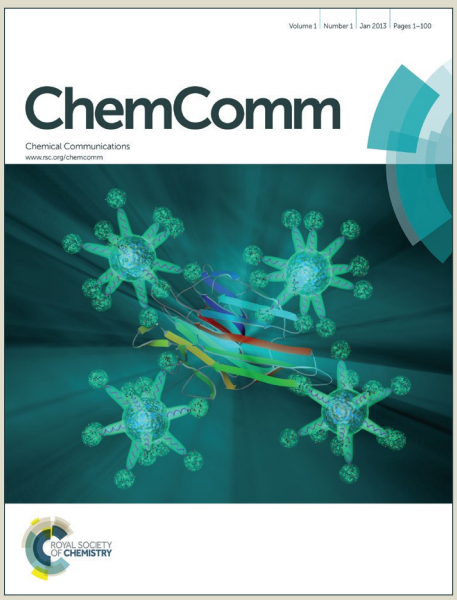

ROYAL SOCIETY OF CHEMISTRY

www.rsc.org/chemcomm

Journal Name

RSCPublishing

COMMUNICATION

Cite this: DOI: 10.1039/x0xx00000x

Received ooth January 2012,
Accepted ooth January 2012

DOI: 10.1039/x0xx00000x

www.rsc.org/

Unification of Catalytic Oxygen Reduction and Hydrogen Evolution Reactions: Highly Dispersive Co Nanoparticles Encapsulated inside Co and Nitrogen co-doped Carbon

Y. Wang, Y. Nie, W. Ding, S. G. Chen, K. Xiong, X. Q. Qi, Y. Zhang, J. Wang, Z. D. Wei*

The Co nanoparticles encapsulated inside Co and nitrogen co-doped carbon catalyst with small particle size and homogenous distribution of Co NPs was elaborately synthesized, which exhibits evidently outstanding activity and stability toward ORR/HER.

The energy crisis and environmental issues have stimulated extensive research on alternative energy storage and conversion systems.[1] Hydrogen is considered as one of the most ideal energy carriers that can be cleanly and efficiently used as fuel in fuel cells. Unfortunately, both oxygen reduction reaction (ORR), the cathode reaction of fuel cells, and hydrogen production reaction from water electrolysis, usually called hydrogen evolution reaction (HER) are sluggish in nature and hence limiting performance of the whole hydrogen-fuel cell-electric systems.[2] Pt and its alloys[3] are widely investigated for ORR and HER due to their high catalytic activities. However their vulnerability and prohibitive cost impede their practical applications. Therefore, it is significant to develop non-precious metal catalysts (NPMCs) with high activity, good retention, low cost and environmental benignancy to replace Pt for both ORR and HER.

Among NPMCs[4], transition metal-nitrogen-containing complexes supported on carbon materials (M−N/C, where M = Fe and Co) are considered to be the most promising alternative for replacing Pt.[5] Nevertheless, the exact nature of the active sites of M−N/C is still under debate and the performance of M−N/C is still required to be improved. Therefore, enormous researches have focused on investigating active sites as well as increasing the density of these sites either by optimizing the nitrogen doping level or the structure of the catalyst. Recently, Zhang al et.[6] demonstrated Co-N_x active sites are closely related to ORR and Atanassov al et.[7] proposed that O_2 is reduced to peroxide on Co-N_x site; Bao al et.[8] reported encapsulating 3d non-precious transition metal nanoparticles (TMNPs) within nitrogen-doped carbon nanotubes (NCNTs) catalysts used for both the ORR and HER. And their experimental results and theoretical calculations demonstrated that the nitrogen-doped graphitic carbon (N-C) surface with metal sitting below is expected to enhance ORR and HER activity due to the decrease of adsorption free energy of O_2 and H*. A Mott−Schottky effect at the metal-doped carbon interface was also possible, further contributed to its potential catalytic event due to its extended electronic structure.[9] Further optimizing the particle size and achieving homogenous distribution of TMNPs in these catalysts may boost the performance of these catalysts. However, since the easily agglomeration and serious sintering of TMNPs at high temperature, at which nitrogen-doped carbon materials are synthesized, the controllable synthesis of composite catalysts containing N-C and homogenous-distributed TMNPs is seldom achieved at the same time. Therefore, it is still desirable yet challenging to synthesize well-dispersed TMNPs and N-C composite for ORR and HER. Herein, we designed and synthesized the highly dispersive Co nanoparticles encapsulated inside Co and nitrogen co-doped carbon catalyst (denoted as Co@Co-N-C) as a bi-functional catalyst for ORR and HER. The highly dispersive active sites rendered by Co@N-C and surface Co-N species were expected to be more effective to catalyze the ORR and HER. Thus this new material has resulted in not only an outstanding catalytic activity similar to Pt/C for ORR at very low cost in alkaline media, but also an excellent HER activity. Moreover, unlike the liner polymers previously used for M−N/C catalysts, Co@Co-N-C catalysts can be utilized as a self-supporting catalyst excluding the use of a carbon support to expose more active sites.

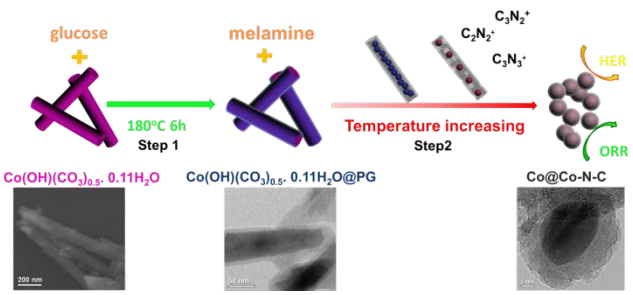

Scheme 1. Synthesis of Co@Co-N-C. Step 1: hydrothermal process; Step 2: thermal treatment process.

The Co@Co-N-C were synthesized by the pyrolysis of $Co(OH)(CO_3)_{0.5}$·$0.11H_2O$@PG (PG: polymerized glucose), which

were prepared by hydrothermally coating the polymeric layer on Co(OH) $(CO_3)_{0.5}$·0.11H_2O nanorods(Fig. 1a), in the presence of melamine, as illustrated in Scheme 1. A representative scanning electron microscopy (SEM) and transmission electron microscopy (TEM) images reveal that the $Co(CO_3)_{0.5}(OH)$·0.11H_2O surfaces are uniformly covered by polymerized glucose with the diameters from 70 to 120 nm and the average thickness of the coating layer is around 9 nm (Fig. 1b-1d). During the Subsequent thermal treatment process, $Co(OH)(CO_3)_{0.5}$·0.11H_2O@PG precursors firstly transformed to CoO@C at low temperature (<500°C). Then under high-temperature (800°C) treatment, the carbon coating layer of CoO@C served as the reductant of CoO and tended to be broken instead of preserving the morphology of Co@C; meanwhile, the nitrogen-containing polymer evolved from melamine was decomposed with simultaneous release of a large amount of carbon nitride gases (e.g., $C_2N_2^+$, $C_3N_2^+$, $C_3N_3^+$), which provided carbon and nitrogen sources to finally evolve into Co@Co-N-C. Due to the protection of polymerized glucose layers, the CoO nanoparticles were expected to be more reluctant to form large aggregates. And the homogeneous mixing of $Co(OH)(CO_3)_{0.5}$·0.11H_2O@PG precursors and melamine marks sure the formation of highly dispersive small Co NPs in Co@Co-N-C.

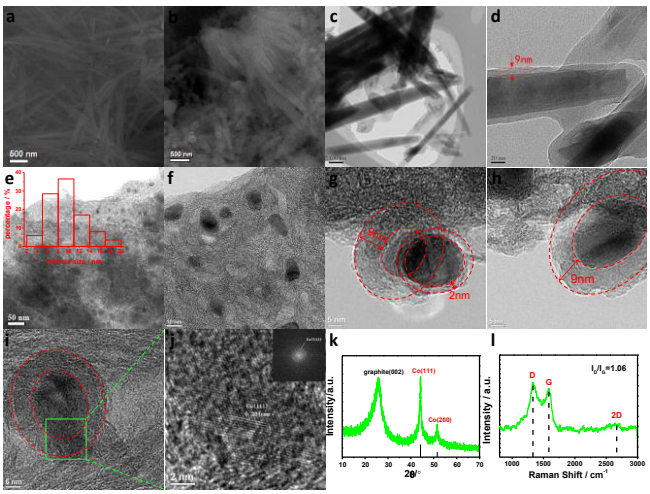

Figure 1. a, b) SEM images of $Co(OH)(CO_3)_{0.5}$·0.11H_2O and $Co(OH)(CO_3)_{0.5}$·0.11H_2O@PG, respectively; c, d) TEM images of $Co(OH)(CO_3)_{0.5}$·0.11H_2O and $Co(OH)(CO_3)_{0.5}$·0.11H_2O@PG; e-i) TEM/HRTEM images of Co@Co-N-C; j) HRTEM images and FFT of Co@Co-N-C; k) XRD patterns for Co@Co-N-C; l) Raman spectrum of Co@Co-N-C.

The morphology and structure of as-synthesized catalysts were characterized by TEM. As shown in 1e and 1f, the highly dispersive small Co NPs (2–20nm) incorporated into the carbon layers are identified and observed. Rarely part of Co NPs -filled carbon nanotubes (CNTs) is also observed (Fig. S1d). High-resolution TEM (HRTEM) images (Fig. 1g and Fig. 1h) show that the Co NPs are coated by 2nm to 9nm graphitic carbon layers. Further HRTEM images (Fig. 1i and 1j) combined with XRD (Fig. 1k) confirm that the cobalt nanoparticles of Co@Co-N-C with a highly crystalline structure of (111) plane are entirely encapsulated within graphitic carbon nanoshells. Additionally, after acid treatment of Co@Co-N-C (denoted as Co@Co-N-C-AT), the XRD pattern in Fig. 4a shows a broad C (002) diffraction peak and the well-defined peaks at around 44.3 °and 51.6 °, which is in good agreement with the characteristics of Co@Co-N-C. Since the pure Co phase is soluble in acid, only protected by carbon layers can it survive in the leaching process, implying that the geometric confinement of cobalt nanoparticles within nitrogen-doped graphitic carbon shells has been successfully synthesized. The Raman spectrum of Co@Co-N-C (Fig. 1i) presents the clearly separated G-band at 1580cm^{-1}, corresponding to graphitic carbon, and the D-band located at 1337cm^{-1}, associated with defects, plus a weak 2D-band peak at 2672cm^{-1}. The relatively high N content which is beneficial to ORR and HER caused that the I_D/I_G ratio of Co@Co-N-C becomes 1.06.

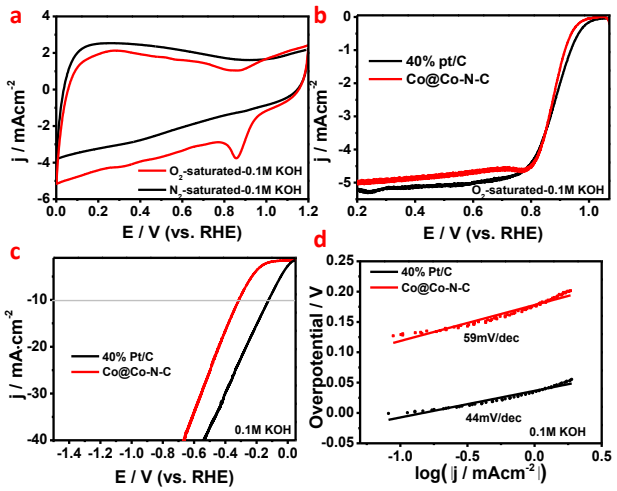

Figure 2. a) CVs for Co@Co-N-C in N_2- and O_2-saturated 0.1 M KOH,; b) ORR LSVs in an O_2-saturated 0.1 M KOH for Co@Co-N-C and 40 wt. % Pt/C at 1600 rpm; c) HER LSVs for Co@Co-N-C and 40wt. % Pt/C in 0.1 M KOH at 1600 rpm, and d) the corresponding Tafel plots in 0.1 M KOH.

To examine the ORR activity of the Co@Co-N-C, cyclic voltammetry (CV) measurement was firstly carried out for Pt/C and Co@Co-N-C in O_2- or N_2-saturated 0.1 M KOH (Fig. 2a). A well-defined ORR peak in O_2-saturated 0.1 M KOH is observed, which is attributed to the electrocatalytic reduction of oxygen on the electrode. The ORR activity of Co@Co-N-C was further quantitatively evaluated with the rotating disk electrode (RDE) measurements. The ORR polarization curve of Co@Co-N-C in O_2-saturated 0.1M KOH exhibits a high onset (ca. 1.020V vs. RHE) and a half-wave potential (ca. 0.879V vs. RHE), both comparable to those of Pt/C catalyst (Fig. 2b) and the state-of-the-art NPMC in alkaline media (Table S1). The HER activity of Co@Co-N-C was also estimated in 0.1 M KOH solution with linear sweep voltammetry (LSV). As shown in Fig. 2c, Co@Co-N-C exhibits excellent electrocatalytic activity for HER. Precisely, Co@Co-N-C exhibits much smaller onset overpotential of 78mV and achieves current densities 10mA cm^{-2} at overpotential of 314mV, superior to some of the best non-noble metal HER catalysts for alkaline media (Table S2). Tafel slopes for Pt/C and Co@Co-N-C are approximately 44 and 59mV dec^{-1}, respectively, revealing that the HER proceeds through a Volmer-Heyrovsky mechanism. Especially, both high performance of Co@Co-N-C for ORR and HER compared with Co@NCNT with sintered Co NPs in extremely irregular size distributed NCNT are observed (Fig. S2, S3), indicating that the highly dispersive Co NPs encapsulated inside Co and nitrogen co-doped graphitic carbon shell is conducive to the high ORR and HER catalytic performance of Co@Co-N-C. Furthermore, Co@Co-N-C shows a remarkable durability for both ORR and HER (Fig. S4-S6). As shown in Fig. S4, accelerated durability test results showed that after 2000 cycles, the half-wave potential for Co@Co-N-C had negatively shifted by 17 mV. For HER, the LSV curves that were measured for Co@Co-N-C catalyst before and after 2000 CV

cycles ranging from 0.2 to -0.2V vs. RHE at a scan rate of 50 mVs^{-1} in 0.1M KOH are shown in Fig. S5. The LSV curve after 2000 CV cycles exhibits negligible loss but an increasing current density at the same potential compared to the initial curve. After 500 CV cycles, the current density increased a little, revealed that the increasing current belongs to the activation and the cleaning of electrode surface. What's more, the Potentiostatic hydrogen evolution reaction was also carried out for Co@Co-N-C catalyst. Only 10% hydrogen evolution current lose after 20000s continuously hydrogen evolution reaction. These results suggest that Co@Co-N-C is of superior activity and stability in a long-term electrochemical ORR and HER process, demonstrating the potential of Co@Co-N-C towards replacing the noble metal based catalysts for highly efficient electrocatalysis of ORR and HER.

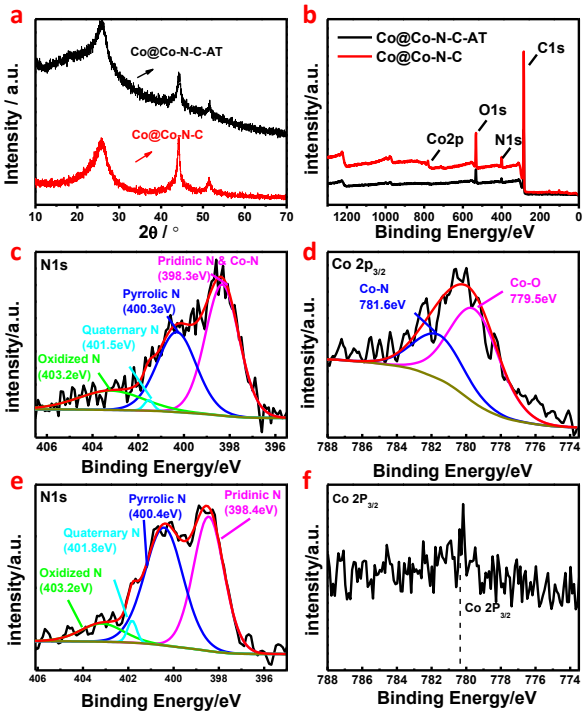

Figure 3. a, b) XRD patterns and XPS spectrum of Co@Co-N-C and Co@Co-N-C-AT; c, d)N1s and Co2p3/2 XPS spectrum of Co@Co-N-C, respectively; e, f)N1s and Co2p3/2 XPS spectrum of Co@Co-N-C-AT, respectively.

In order to distinguish the possible effect of Co@N-C and surface Co-N species, we attempted to remove the surface Co-N species with hot sulfuric acid. The well-preserved Co NPs in the graphitic carbon of Co@Co-N-C after the leaching process is demonstrated as mentioned before. The forms of surface Co for Co@Co-N-C are Co-O and Co-N[10] (Fig. 3d); while the negligible surface cobalt content (Fig. 3f) and the decreased content of overlapping pyridinic N and Co-N bonding[10b] (Fig. 3b, 3d, Table S3, S4) exist on the surface of Co@Co-N-C-AT, signifying that surface Co-N species are removed entirely. Since the electrochemical performance of the Co@Co-N-C-AT was slightly inferior to that of the Co@Co-N-C in Fig. S7, it can be proposed that the surface Co-N species maybe one type of active sites. Despite the decrease of ORR and HER activities after acid treatment, Co@Co-N-C-AT still has a relatively high ORR and HER activities in 0.1M KOH compared to those of Co@NCNT (Fig. S8), which could be attributed to the highly dispersive active sites of Co@N-C. This results coupled with the recent studies on M−N/C or M-containing NCNTs and Mott−Schottky effect for electrocatalysis, as shown in Fig. 4, we believe that the electronic structure of the outermost nitrogen doped carbon layer is modulated by electronic interaction and electron transfer between the metal and cobalt core and nitrogen doped carbon layer. This re-distribution of electrons of Co, C and N atoms excites nitrogen-doped carbon shell domains adjacent to small Co NPs, which further enhances the electrocatalytic activity for ORR and HER. Accordingly, a cooperative and/ or synergistic catalytic effect between the surface Co-N species and Co@N-C in Co@Co-N-C can be proposed to account for the high performances of Co@Co-N-C.

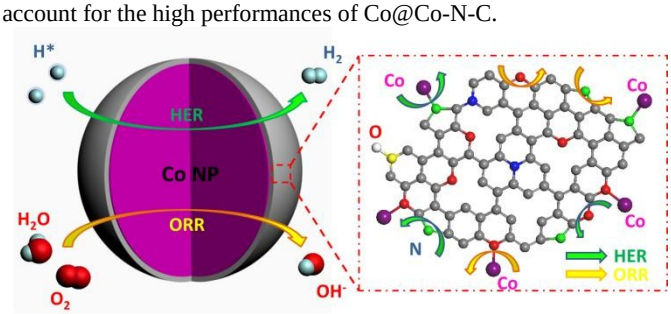

Figure 4. The catalyst mechanism of Co@Co-N-C catalyst.

Conclusions

In summary, a highly dispersive Co NPs @ Co-N-C with excellent ORR and HER activity and stability has been successfully synthesized. The superior electrocatalytic activity is attributed to the dual active sites composed of nitrogen-doped carbon shell domains adjacent to small Co NPs and the highly active surface Co-N species. As a result, this non-precious metal catalyst can be a promising potential alternative for Pt/C, and the scalable synthesis of Co@Co-N-C with low cost and environmental benignancy will have a significant impact on the development of hydrogen-fuel cell-electric systems involving ORR and HER.

This work was financially supported by the China National 973 Program (2012CB720300 and 2012CB215500), by the NSFC of China (Grant Nos. 21436003 and 21176271)

Notes and references

The State Key Laboratory of Power Transmission Equipment & System Security and New Technology, College of Chemistry and Chemical Engineering, Chongqing University, Chongqing,400044 (China)
Fax: +86 23 65102531;
E-mail: zdwei@cqu.edu.cn (Wei);

† Electronic Supplementary Information (ESI) available: the details of experimental procedures, electrochemical tests, stability test, methanol tolerance tests. See DOI: 10.1039/c000000x/

1 a) F. Cheng, J Chen, *Chem. Soc. Rev.*, 2012, **41**, 2172–2192; b) Y. Nie, L. Li, Z. Wei, *Chem. Soc. Rev.*, 2015, **44**, 2168-2201; c) T. Y. Ma, S. Dai, M. Jaroniec, S. Z. Qiao, *J. Am. Chem. Soc.*, 2014, **136**, 13925–13931; d) S. Chen, J. Duan, W. Han, S. Z. Qiao, *Chemical Communications*, 2014, **50**, 207-209; e) Y. Zheng, Y. Jiao, M. Jaroniec, S. Z. Qiao, *Angew. Chem. Int. Ed.*, 2015, **54**, 52-65.

2 a) C. Chen, Y. Kang, Z. Huo, Z. Zhu, W. Huang, H. L. Xin, J. D. Snyder, D. Li, J. A. Herron, M. Mavrikakis, M. Chi, K. L. More, Y.

Li, N. M. Markovic, G. A. Somorjai, P. Yang and V. R. Stamenkovic, *Science*, 2014, **343**, 1339-1343; b) P. Jiang, Q. Liu, Y. Liang, J. Tian, A. M. Asiri and X. Sun, *Angewandte Chemie*, 2014, **53**, 12855-12859; c) J. W. D. Ng, M. H. Tang, and T. F. Jaramillo, *Energy Environ. Sci.*, 2014, **7**, 2017-2024;

3 a) Y. Nie, S. Chen, W. Ding, X. Xie, Y. Zhang and Z. Wei, *Chemical communications*, 2014, **50**, 15431-15434; b) S. Chen, Z. Wei, X. Qi, L. Dong, Y. G. Guo, L. Wan, Z. Shao and L. Li, *Journal of the American Chemical Society*, 2012, **134**, 13252-13255; c) S. I. Choi, M. Shao, N. Lu, A. Ruditskiy, H. C. Peng, J. Park, S. Guerrero, J. Wang, M. J. Kim and Y. Xia, *Acs Nano*, 2014, **8**, 10363-10371; d)W. Sheng, H. A. Gasteiger and Y. Shao-Horn, *Journal of The Electrochemical Society*, 2010, **157**, B1529.

4 a) Y. Wang, W. Ding, S. Chen, Y. Nie, K. Xiong and Z. Wei, *Chemical communications*, 2014, **50**, 15529-15532; b) W. Ding, Z. Wei, S. Chen, X. Qi, T. Yang, J. Hu, D. Wang, L. J. Wan, S. F. Alvi and L. Li, *Angewandte Chemie*, 2013, **52**, 11755-11759; c) J. Liang, R. F. Zhou, X. M. Chen, Y. H. Tang and S. Z. Qiao, *Advanced materials*, 2014, **26**, 6074-6079; d) K. Zhang, X. Han, Z. Hu, X. Zhang, Z. Tao, J. Chen, *Chem. Soc. Rev.*, 2015, **44**, 699-728. e) R. Zhou, S. Z. Qiao, *Chemical Communications*, 2015, DOI: 10.1039/C5CC00995B.

5 a) M. Lefevre, E. Proietti, F. Jaouen and J. P. Dodelet, *Science*, 2009, **324**, 71-74; b) R. Jasinski, *Nature*, 1964, **201**, 1212-1213; c) N. Ranjbar Sahraie, J. P. Paraknowitsch, C. Gobel, A. Thomas and P. Strasser, *Journal of the American Chemical Society*, 2014, **136**, 14486-14497; d) G. Wu, K. L. More, C. M. Johnston and P. Zelenay, *Science*, 2011, **332**, 443-447; e) X. Zou, X. Huang, A. Goswami, R. Silva, B. R. Sathe, E. Mikmekova and T. Asefa, *Angewandte Chemie*, 2014, **53**, 4372-4376. f) J. Du, F. Cheng, S. Wang, T. Zhang, J. Chen, *Sci Rep*, 2014, **4**, 4386.

6 Q. Liu and J. Zhang, *Langmuir : the ACS journal of surfaces and colloids*, 2013, **29**, 3821-3828.

7 a) T. S. Olson, S. Pylypenko, P. Atanassov, K. Asazawa, K. Yamada, *J. Phys. Chem. C*, 2010, **114**, 5049; b) T. S. Olson, S. Pylypenko, J. E. Fulghum, *J. Electrochem. Soc.*, 2010, **157**, B54.

8 a) J. Deng, P. Ren, D. Deng, L. Yu, F. Yang and X. Bao, *Energy & Environmental Science*, 2014, **7**, 1919; b) D. Deng, L. Yu, X. Chen, G. Wang, L. Jin, X. Pan, J. Deng, G. Sun and X. Bao, *Angewandte Chemie*, 2013, **52**, 371-375.

9 X. Li, M. Antonietti, *Chem. Soc. Rev.*, 2013, **42**, 6593-6604.

10 a) Z. S. Wu, L. Chen, J. Liu, K. Parvez, H. Liang, J. Shu, H. Sachdev, R. Graf, X. Feng and K. Mullen, *Advanced materials*, 2014, **26**, 1450-1455; b) H. W. Liang, W. Wei, Z. S. Wu, X. Feng and K. Mullen, *Journal of the American Chemical Society*, 2013, **135**, 16002-16005.

